Journal of Harbin Engineering University Vol 44 No. 7
ISSN: 1006-7043 July 2023

Study Of EDM Properties of Reinforced Cryogenic Treated Aluminum Alloy AA6063 Composites

S. Prakasam*, P. Thangavel, K. M. Arunraja, S. Meinathan

Shree Venkateshwara Hi-Tech Engineering College, Gobichettipalayam, Erode-638455, Tamilnadu.

*Corresponding Author: sphodmech@gmail.com

ABSTRACT

Materials are in high demand because of the constant force to enhance the functionality of structural, aeronautical, and automotive parts. Consequently, it motivates the discovery and manufacture of composite materials. Aluminum metal matrix composites employ in the automotive and aerospace industries due to their high strength-to-weight ratio and wide range of acceptable mechanical and tribological qualities. This study analyzed the surface sticks of AA6063-B_4C composites that cryogenically treatfor their ED machining capabilities. Stir casting is one of the liquid metrological methods employed to create B_4C particle-reinforced aluminum metal matrix composites—different soaking times in liquid nitrogen on the samples (13, 26 & 39 hours). Various inputs, such as soaking time (SoT), electrode gap (Gap), Current, Pon (Pulse ON time), and Poff (Pulse OFF time), were studied about the outputs of material removal (MR) rate, tool wear (TW) rate, and surface roughness (Ra). It observesby experiment that Current is one of the most influential parameters for ED machining.

Keywords: AA6063, B_4C, soaking time, Pulse ON time, Pulse OFF time, MR rate, L27 orthogonal array

1. INTRODUCTION

The medical, automotive, and aerospace industries have recently increased their demand for structural materials, focusing on weight[1]. Car manufacturers have begun using lighter-weight materials to save money at the gas pump. Aluminum alloys are crucial in modern industries because of their low density, high strength, high corrosion resistance, and outstanding thermal surface sticks[2], [3]. Aluminum alloys strengthened with rigid materials produce composites with superior strength and improved features. The material's mechanical and thermal properties improve if reinforcement particles add to a base metal alloy[4], [5].

Aluminum metal matrix composites (Al-MMC) typically use Al_2O_3, B_4C, SiC, TiB_2, and Mg as reinforcement particles due to their unique properties[6]. Low density, higher strength-to-weight ratio, wear-based resistances, lower chemical reactions, etc., make it ideal for producingaviation and automotive components[7]. It isnot easy to machine these materials using traditional methods because of how well they stick together.

Before CNC, traditional machining operations relied on a shearing approach to remove material[8]. Higher interface temperatures achieve during the shearing process by creating an interface between the workpiece (W/P) and the tool (T)[9], [10]. This high temperature causes premature tool failure, poor surface polish, and a lack of dimensional precision in the finished components[11], [12]. These issues have prompted many sectors to use alternative machining techniques[13]. Table 1 summarizes the many kinds of unconventional machining techniques[14], [15]. Electrical discharge machining is a subset of the unconventional machining techniques used for working with electrically conductive hard materials (ED machining)[16]. Thermoelectric energy employs to extract the material from W/P in this machining process. Electrical discharge energy at a high frequency erodes the material by creating a gap between two spatially separated electrodes (one T and one W/P). Dielectric fluid utilizes to cool the

electrode and W/P and to flush away eroded particles that have fallen in the spaces between the electrodes [17], [18]. ED machining can process various parts, including those with intricate details and irregular contours, such as those used in the aerospace and medical industries, and forging tools, press tools, extrusion dies, and internal components with detailed profiles[19]. ED machining displays excellent dimensional precision for complex design components. ED machining is used in the aerospace industry to create intricate profile dies and associates [20].

Table 1. Non-conventional machining process.

1 Mechanical machining	a. Abrasive Jet Machining (AJM)
	b. Ultrasonic Machining (USM)
	c. Water Jet Machining (WJM)
	d. Abrasive Water Jet Machining (AWJM)
2 Chemical Machining	a. Chemical Milling (CM)
	b. Petro Chemical Milling (PCM)
3 Electro-Chemical machining	a. Electro Chemical Machining (ECM)
	b. Electro Chemical Grinding (ECG)
	c. Electro Jet Drilling (EJD)
4 Electro - Thermal Machining	a. Electro Discharge Machining (EDM)
	b. Laser jet Machining (LJM)
	c. Electron beam Machining (EBM)

The figures in Figures 1 and 2 show the ED machining process, with the variables that affect the performance and quality of the methodoffered. Therefore, the primary objective of ED machining is to maximize the I/P and O/P values. The procedures' final results explain the MR rate, TW rate, Ra, and radial overcut. Brass and Copper are used as electrodes in electrical discharge machining because they have high electrical conductivity[21]–[23]. Graphite's high melting point, strong wear resistance, and conductivity make it a popular choice as an electrode material for many tools [24]. This paper first discusses the history of studies on ED machining of metal matrix composites, then details the considerations that went into the study, and lastly presents the experimental design and results of a Taguchi analysis.

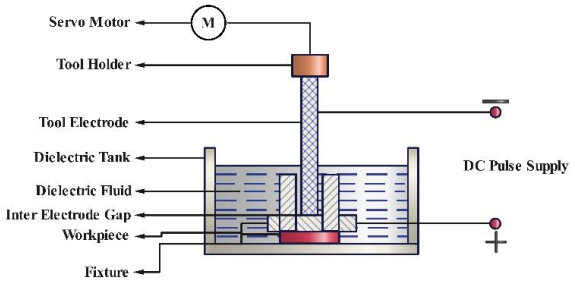

Figure 1. EDM setup.

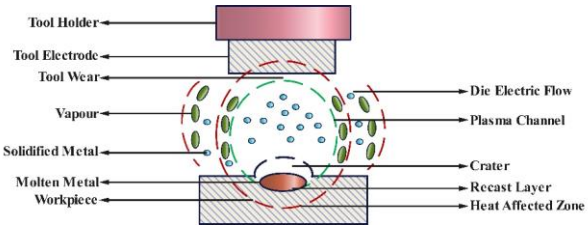

Figure 2. EDM Process.

By employing the stir casting technique, researchers created MMC samples based on AA6063 –B_4C. Machining rates (MR and TW) and other parameters are studied and compared to those achieved by traditional and rotary ED machining[25]. For both ED machining procedures, a machining time of 10 minutes and a variety of additional parameters, including Current (3, 5, 7, 9, 11), pulse time (50, 100, 150, 200, 250), and duty cycle (0.50, 0.55, 0.60, 0.65, 0.70), are considered. The tool rotation speed in rotary ED machining is held constant at 500 rpm. The MR and TW rates decreased with increasing pulse time. Boosting the current and the duty cycle raises the MR and TW rates, respectively[26]. The MR rate and Electrode wear rate of rotational ED machining is reduced compared to traditional ED machining [27], [28].

Input parameters (Current, gap voltage, Pon, Poff, and fluid pressure) study by the author of[29] found that Current and Pon strongly influence both MR rate and TW rate during ED machining of AA6063 material. The fluid pressure, current, Poff voltage, and gap voltage contribute to the aforementioned geometrical flaws. Researcher of[30]analyzed the parameters of the ED machining process using AA6063 as the work material. Peak current (6, 12, 18V), Voltage gap (50, 60, 70), Pon (75, 100, 150s), Flushing pressure (0.5, 0.7, 0.9 kgf/cm 2), and machining depth as 0.5mm were taken into account for this analysis. The MR rate, the L27 OA, and ANOVA methods employ to analyze the data, and the ANN utilizes to find the optimal model. Current (80, 120, 160V), Pon (110, 115, 120s), and Poff (40, 50, 60Hz) employ during Wire cut ED machining of 10% TiO_2 particles supplemented via stir casting with AA6063. The study found that Current -150A, Pon -112s, and Poff -50s provided the best values for MR rate and Ra. Current (51.96%), Pon (34.59%), and Poff (12.21%) dominate the output parameters, and 42.8% of the composite preference was reached [31].

The effect of machining factors on ED machining of AA6063 in both stationary and rotary modes analyze, and it initiates that the MR rate and Ra are more significant in the latter[32], [33]. There is a correlation between Poff, Spark gap, and MR rate [34], and Poff, peak current, and a correlation to Ra. The output parameters of ED machining analyze after being applied to constructed B_4C reinforced AA6063 MMC. The results, which used a copper rod as the tool electrode, show that the TW rate and current affect the MR rate and Ra as a function of the tool life. Pon affects how researchers [35]evaluate how well the ED machining process performs. The effect of ED machining input parameters on red mud-reinforced AA6063 metal matrix composite output parameters examines by the author of [36]. After considering all of the input parameters used in ED machining, the author [37]has determined that discharge current and Pon are the two most crucial. To create AA6061 MMC, 10% Al2O3 was used in a stir casting method. Machining parameters included a Discharge current of 6, 10, 14 A, a Pon of 75, 100, and 200s, and a Duty factor of 50, 60, and 70, respectively, to produce the desired results in the samples using ED machining. The Taguchi method employs to achieve optimality in experimental design and provide conclusions about the relationship between the parameters [38].

An LM6 aluminum metal matrix alloy was stir-cast with Al_2O_3 particles added at a 10% reinforcement level. Due to considerationof the operating parameters and the samples were machined using ED machining. The most critical factors, in this case, are outlined by Taguchi basis of L27 OA [39]. Author of[40]experimented on fabricating AA6061 MMC with SiC and Gr particle inclusions via stir casting. From those results, they derived a mathematical model relating to the operating and used the ANOVA method to analyze the significance of those parameters. The MR rate, TW rate, and Ra parameters were all found to be affected by the input parameters. Taguchi analysis determines the optimal input parameters for ED machining of AlSi 10Mg hybrid metal matrix composites with Alumina and Graphite reinforcement. The MR and TW rates were affected by flushing pressure [41].

The current study of cryogenically treated AA6063-B_4C metal matrix composite involved experimenting with machining factors such as Cryogenic soaking time, Electrode Gap, Current, Pon, and Poff from earlier literature. Components such as aircraft fittings, missile parts, cooking utensils, window frames, and bicycle frames can all fabricate using this composite.

2. MATERIAL AND PREPARATION

Aluminum metal matrix composites can be stir-cast in various manufacturing processes, and the method is simple and cost-effective. In Table 2,researchers see AA6063's chemical composition. The most challenging reinforcing particles blend in a stir casting technique at the molten stage. Figure 3 depicts the stir casting setup, and Table 3 lists some key process parameters. Matrix AA 6063 is cut into pieces and tossed into the oven. It is heated in a furnace to just over its melting point to liquefy

the matrix material completely. To reinforce the metal in this research, 6% boron carbide add after heating to 350°C. After the matrix material heat to a liquid state, the particles are added and stirred constantly for up to three or four minutes to ensure a thorough mixture. Pouring the molten metal mixture into the mold produces a composite specimen that can be removed from the mold once it has cooled. The guaranteed minimum size of the solidified example is 100 mm on all sides and 10 mm in thickness. The samples are thoroughly cleaned after mechanical testing and immersed in deep cryogenic treatment for 13, 26, or 39 hours.

Table 2. Chemical composition ofAA 6063.

Materials	Si	Fe	Mn	Mg	Cr	Zn	Ti	Al
Wt %	0.63	0.83	0.069	0.38	0.017	0.16	0.029	remaining

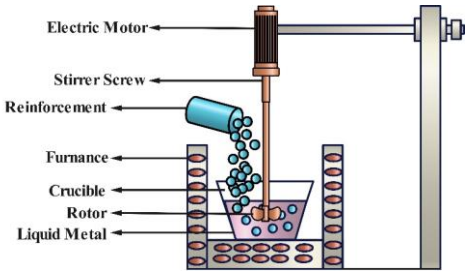

Figure 3. Stir casting setup.

Table 3. Stir casting processingfactors.

S.No	Factors	Value
1	Stirring time (min)	5
2	The preheated temperature of reinforcement particles (°C)	900
3	Blade angle (°)	30
4	Spindle speed(rpm)	650

3.1 Selection of Design Factors

Pulse ON time, Pulse OFF time, duty factor, machining voltage, polarity, discharge gap, and die electric fluid flushing pressure are only some of the machining parameters selected for study throughout the ED machining process. Evaluation of the ED machining procedure concerning the MR rate, the TW rate, and the quality of the machined surface. The following variables -are taken into account in this experimental study (i)SoT for W/P; (ii) Pon; (iii) Gap; (iv) Poff; and (v) Current. Table 4 lists the control factors and their corresponding values throughout the various levels. Table 5 shows the experimental layout that develops using the values of the control variables.

Table 4. Control factors and their values.

Code of Input Parameters	Input Parameters	Unit	Representation	Level 1	Level 2	Level 3
A	Soaking Time	Hrs	Time duration of cryogenic treatment of W/P material	13	26	39
B	Electrode Gap	mm	The gap between the tool electrode and W/P electrode	0.3	0.6	0.9

C	Current	A	The maximum intensity of discharge current	70	110	150
D	Pulse ON Time	ms	Allowed period for current flow in the electrode and W/P	130	140	150
E	Pulse OFF Time	ms	Interval time between the successive spark	80	90	100

Table 5. Processingfactors with specified levels.

S. No	A	B	C	D	E
1	1	1	1	1	1
2	1	1	1	1	2
3	1	1	1	1	3
4	1	2	2	2	1
5	1	2	2	2	2
6	1	2	2	2	3
7	1	3	3	3	1
8	1	3	3	3	2
9	1	3	3	3	3
10	2	1	2	3	1
11	2	2	2	3	2
12	2	2	3	1	3
13	2	2	3	1	1
14	2	2	3	1	2
15	2	2	3	1	3
16	2	3	1	2	1
17	2	3	1	2	2
18	2	3	1	2	3

19	3	1	3	2	1
20	3	1	3	2	2
21	3	1	3	2	3
22	3	2	1	3	1
23	3	2	1	3	2
24	3	3	1	3	3
25	3	3	2	1	1
26	3	3	2	1	2

3.2 Response Variables

The MR rate, the TW rate, and the Surface roughness are the productivity and efficiency indices of the ED machining process. Three factors determine how effective ED machining is. (i) Erosion of the W/P per time unit is equivalent to the MR rate. The experimental study by author [42]uses two response variables, (ii) TW rate, which stands for total off material wearing out of tool electrode per unit time, and (iii) Ra - Surface roughness, which stands for abnormalities in the machined surface texture. The properties of (i) carbon breakdown and deposition, (ii) debris concentration, and (iii) plasma growth determine the MR and TW rates, respectively. The machining rate (MR) and the tool wear rate (TW) evaluates by comparing the pre-and post-machining weights of the workpiece (W/P) and the tool electrode. Weighing the W/P and the electrode with a 0.001g accuracy accomplish with the help of computerized weighing equipment. The surface roughness tester calculates Ra values. The MR and TW rates were determined using equations (1) and (2).

$$MR\text{rate}=\frac{W_{\text{before}}-W_{\text{after}}}{t_{\max}}\cdot\frac{1}{\rho} \quad (1)$$

$$TW\text{rate}=\frac{E_{\text{before}}-E_{\text{after}}}{W_{\text{before}}-W_{\text{after}}} \quad (2)$$

Whereas

W_{before} W_{after} indicates weightage of workpiece material beforehand and afterward machining (g)

t_{max}indicates machining time (min)

ρshowsthe density of workpiece material

E_{before} E_{after}indicatesweightage of the electrode before and after machining correspondingly.

4. EXPERIMENTAL METHOD

Taguchi used a three-factor, three-level design in this experimental study. Table.6 shows the number of trials conducted with different permutations. The DOE factors sort, and the resulting rows number four, five, and six. Look at these numbers in terms of the machining process's settings. Three "Smaller the better" and "Nominal the better" in the analysis "better" is chosen for MR rate and "Smaller the better" optimal machining input parameters based on the SN ratio.

According to the Taguchi technique, the method is the best choice when determining the optimal number of experiments to run. An investigationusing L27 OA with a three-factor, three-level design, considering the input and output parameters. The results of the tests with different combinations of input parameters in Table 6, where the columns describe the

parameters themselves and the rows detail the number of times each combination experiment. The parameters using the DOE and the resulting experimental output parameters place in the fourth, fifth, and sixth columns. Optimize the ED machining process by analyzing the data in the ANOVA table. Parameters for the machining process. There are three possible rankings in the analysis depending on the SN ratio: "Larger is better," "Smaller is better," and "Nominal is better." For best machining input factors, this experiment chooses "Larger is better" for MR rate and "Smaller is better" for TW rate and Ra.

In the Taguchi method, Larger is better calculated based on the equation (3),

$$\eta = -10\log\left[\frac{1}{n}\sum_{l=1}^{n} Y_i^{-2}\right] \quad (3)$$

In the Taguchi method,smaller is better calculated based on the equation (4),

$$\eta = -10\log\left[\frac{1}{n}\sum_{i=1}^{n} Y_i^{2}\right] \quad (4)$$

Where

ηdenotesthe SN ratio

$n$indicatesa repeated number of each experiment

$i$denotes experiment number

Yrepresents observed value in i^{th} experiment

Table 6. L27 orthogonal array experimental design &its results.

S.No	Input factors					Output factors		
	A	B	C	D	E	MR_{rate}	TW_{rate}	Ra
						g/min	g/min	mm
1	13	0.3	70	130	80	0.5171	0.0016	3.931
2	13	0.3	70	130	90	0.5121	0.0017	3.922
3	13	0.3	70	130	100	0.5091	0.0015	3.918
4	13	0.6	110	140	80	0.5787	0.0028	4.727
5	13	0.6	110	140	90	0.5751	0.0029	4.724
6	13	0.6	110	140	100	0.5704	0.0027	4.708
7	13	0.9	150	150	80	0.6221	0.0063	5.331
8	13	0.9	150	150	90	0.6181	0.0072	5.321
9	13	0.9	150	150	100	0.6116	0.0062	5.316
10	26	0.3	70	150	80	0.5288	0.0045	4.141
11	26	0.3	70	150	90	0.5266	0.0045	4.125
12	26	0.3	70	150	100	0.5234	0.0043	4.119
13	26	0.6	110	130	80	0.5653	0.0049	5.289
14	26	0.6	110	130	90	0.5628	0.0047	5.229
15	26	0.6	110	130	100	0.5602	0.0046	5.221
16	26	0.9	150	140	80	0.5379	0.0033	5.296

17	26	0.9	150	140	90	0.5353	0.0033	5.293
18	26	0.9	150	140	100	0.5335	0.0032	5.293
19	39	0.3	70	140	80	0.5649	0.0059	4.414
20	39	0.3	70	140	90	0.5622	0.0059	4.388
21	39	0.3	70	140	100	0.5604	0.0058	4.383
22	39	0.6	110	150	80	0.5459	0.0033	4.533
23	39	0.6	110	150	90	0.5428	0.0033	4.529
24	39	0.6	110	150	100	0.5390	0.0032	4.521
25	39	0.9	150	130	80	0.5933	0.004	4.938
26	39	0.9	150	130	90	0.5897	0.004	4.929
27	39	0.9	150	130	100	0.5852	0.004	4.915

5 RESULTS AND DISCUSSION

The ANOVA technique in MINITAB analyzes the statistical data collected during the experiment. Key inputs that significantly impact outcomes identify by this research and explain below.

5.1 Analysis of Variance (ANOVA)

The F test evaluates the relevance of the machining factors and the optimum combination level of parameters. An analysis of variance is employed to assess the output data produced from the experimental data. The Taguchi approach uses experiments to determine the best settings for each ED machining process parameter. The process's inherent variability diminishes by analyzing each input parameter's consequences concerning the chosen output parameters. The researchers played around with different permutations and combinations of the variables' means and SN ratios. The ANOVA technique analyzes the statistical significance of the input parameters influencing MR rate, 'TW rate, and Ra. In this investigation, researchers use a significance level of 0.5 (99.5% confidence). F-value from the ANOVA table was used to determine the importance of the effect. The response parameter with the most significant F value is the most influential. It emphasizes in the following sections for the discussion of the MR rate, the TW rate, and the Ra that an analysis of variance of Mean, SN ratio, and response tables of them generated.

5.2 Material Removal Rate (MR rate)

The higher the MR rate, the more debris cleared from the water every minute; hence the better. Table 7 displays the SN ratio value estimated for the MR rate, the ANOVA results, and its response tothe mean MR rate based on the experimental data. Due to the significant energy input for the high current value, the MR rate fluctuates linearly with the present, as shown in Figures 4 (a & b). Depending on the delta value, the MR rate output parameter is most affected by three parameters: (i) Current, (ii) Gap, and (iii) SoT, in that order. Table 9 displays the ANOVA for MR rate means. The current F value is the highest in this table, followed by the Gap and the SoT values.

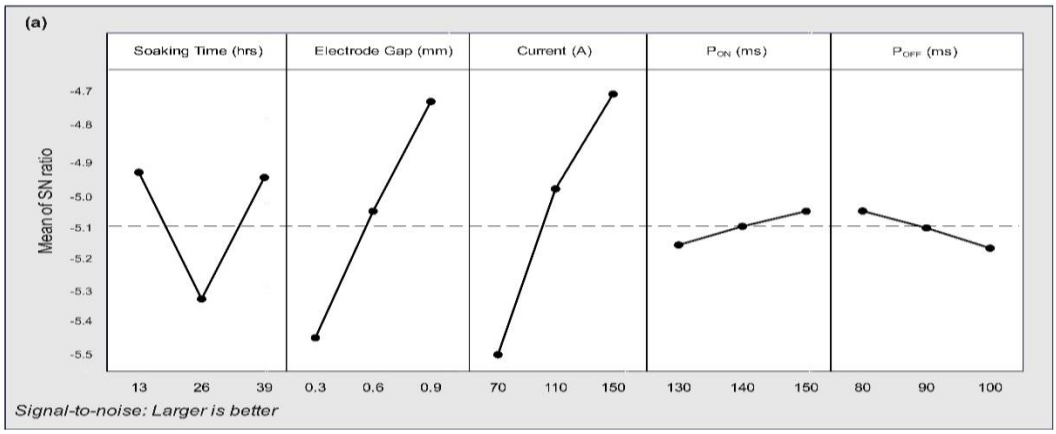

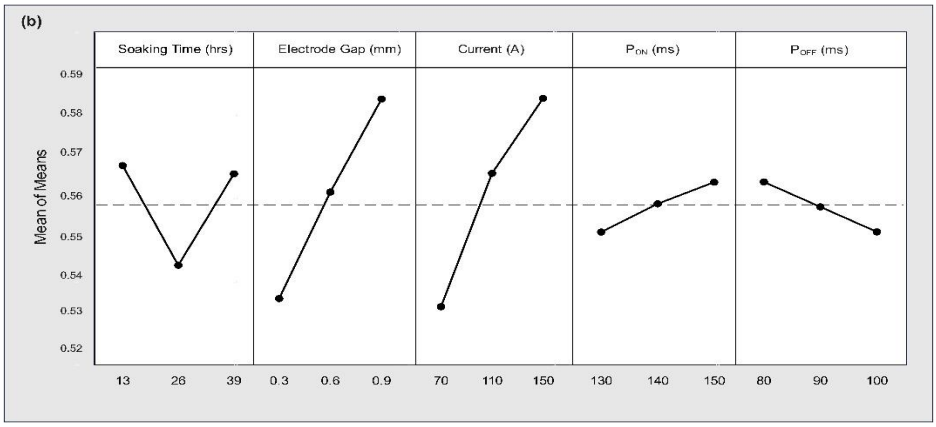

Figure 4. MR rate main effect plot – SN ratio (a). MR rate main effect plot - means (b).

Tables 7 and 9 of ANOVA show that the current F value is greater than the other variables. Table 10 shows that Current, Gap, and SoT are the order of importance for influencing the MR rate based on the delta value. The results show that Pon and Poff had the slightest bearing on the MR rate. Figure 4(a & b) shows the SN ratio and Means of input parameters that affect the MR rate and their relationship to the MR rate, Current, Pon and Poff, Gap, and SoT. The graph illustrates that the MR rate and Gap and Pon have been rising recently. The MR rate interaction plot indicates in Figure 5. For these specific values of SoT(13 Hrs), Gap(0.9 mm), Current(150 A), Pon(150 ms), and Poff (80 ms), the best MR rate is determined.

Table 7. Analysis ofvariance for SN ratio ofMR rate.

Source	DF	Seq SS	Adj SS	Adj MS	F	P
A	2	0.86410	0.86410	0.43216	2027.62	0
B	2	2.38428	2.38428	1.19194	5597.56	0
C	2	2.87876	2.87876	1.43948	6759.91	0
D	2	0.04884	0.04884	0.02451	114.96	0
E	2	0.04913	0.04913	0.02451	115.53	0

Residual Error	16	0.00416	0.00416	0.00032		
Total	26	6.22927				

5.3 Tool Wear Rate (TW rate)

Tool wear occurs naturally during ED machining. Tool wear reduces the precision of the machined surface in terms of its geometrical accuracy. In the ED machining process, the tool electrode and the workpiece (W/P) are both machined away. Carbon and other fluid-borne (dielectric) constituents wrap up the electrode surface and slow the TW rate. Experiment-based analysis of variance for the SN ratio of TW rate indicates in Table 11. This table's F value means that the current input parameter has the most impact on the TW rate, followed by the Pon and cryogenic SoT, and then by the Gap and Poff, which have the most negligibleeffect on the TW rate. Based on the more considerable delta value presented in Table 12, the SN ratio's response table provides information regarding the input parameters that affect the TW rate. The input parameters rank from best to worst based on the delta value: (i) current, (ii) Pon and (iii) SoT. Table 13 displays an ANOVA performed on the means of experimental data for TW rate. The factors with the highest F values in this table affect the TW rate. According to the data in the table, Current and Pon both significantly affected the TW rate.

Table 8. S/N ratio's response table

Level	A	B	C	D	E
1	−4.952	−5.472	−5.521	−5.138	−5.033
2	−5.341	−5.053	−4.998	−5.09	−5.09
3	−4.972	−4.741	−4.75	−5.031	−5.135
Delta	0.393	0.732	0.791	0.105	0.104
Rank	3	2	1	5	4
Larger is better					

Table 9. ANOVA for MRR (mean).

Source	DF	Seq SS	Adj SS	Adj MS	F	P
A	2	0.003812	0.003812	0.001887	1709.9	0
B	2	0.009996	0.009996	0.00499	4539.31	0
C	2	0.011912	0.011912	0.005962	5413.41	0
D	2	0.00031	0.00031	0.000118	105.52	0
E	2	0.000211	0.000211	0.000103	93.61	0
Residual Error	16	0.000019	0.000019	0.000002		
Total	26	0.02626				

Table 10. Mean's response table.

Level	A	B	C	D	E
1	0.5681	0.5341	0.5602	0.5551	0.5624
2	0.5417	0.5598	0.5735	0.5582	0.561
3	0.5651	0.5807	0.5907	0.5625	0.5553
Delta	0.0272	0.052	0.0609	0.0079	0.0071
Rank	3	2	1	4	5

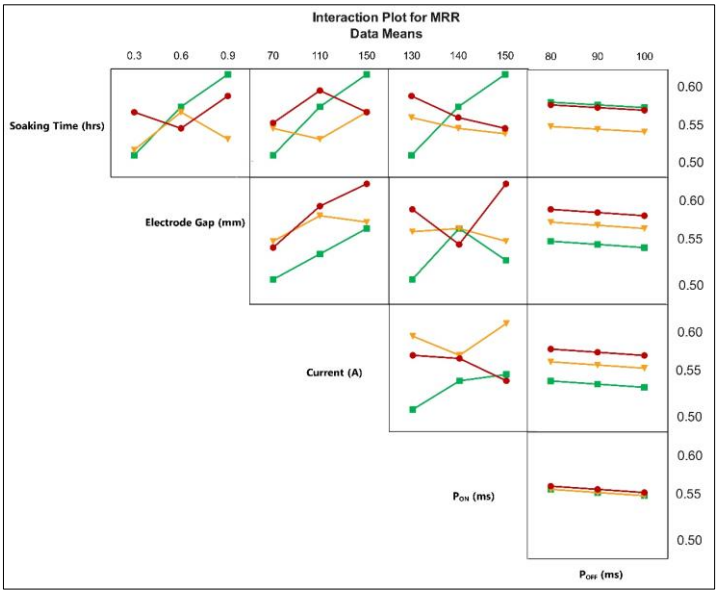

Figure 5. MRR's interaction plot.

Table 11. ANOVA for S/N ratio for TWR.

Source	DF	Seq SS	Adj SS	Adj MS	F	P
A	2	41.225	41.225	21.219	1467.32	0
B	2	9.981	9.981	4.991	358.29	0
C	2	227.82	227.82	114.372	8169.13	0
D	2	77.98	77.98	39.496	2774.31	0
E	2	0.472	0.472	0.242	17.72	0
Residual Error	16	0.223	0.223	0.015		
Total	26	357.701				

Table 12. S/N ratio's response table (TWR)

Level	A	B	C	D	E
1	51.32	50.24	53.04	52.28	49.16
2	49.12	49.86	50.21	49.46	50.01
3	49.56	49.04	46.34	48.34	50.31
Delta	3.26	2.19	8.0	5.1	0.4
Rank	3	4	1	2	5
Smaller is better					

Table 13. ANOVA for TWR (means)

Source	DF	Seq SS	Adj SS	Adj MS	F	P
A	2	0.000003	0.000003	0.000001	454.64	0
B	2	0.000003	0.000003	0.000001	403.06	0
C	2	0.000043	0.000042	0.000021	9582.81	0
D	2	0.00002	0.00001	0.000005	2369.53	0
E	2	0	0	0	16.51	0
Residual Error	16	0	0			
Total	26	0.000056				

Table 14. Mean's response table (TWR)

Level	A	B	C	D	E
1	0.003441	0.003851	0.0027	0.003039	0.003871
2	0.004042	0.003491	0.003324	0.003871	0.003838
3	0.003981	0.004113	0.005524	0.004546	0.003745
Delta	0.0007	0.000624	0.002924	0.001512	0.000123
Rank	4	3	1	2	5

The response table for means shows the order of the most influential factors on the TW rate. Table 14 contains the relevant information. The sequence is (i) Current (ii) Pon (iii) Gap. The central impact plot for mean and SN ratio of tool wear ratio (Figure 6a & b) displays the factors that affect the TW rate. TW rate interaction diagram depicts in Figure 7. Due to the significant thermal

energy produced between the electrode and the W/P, melting and vaporizing happened in the machining region. For this reason, an increase in Current leads to a higher TW rate because a more significant amount of material is from the electrode at a given MR rate. When the following process parameters employ: SoT (13 Hrs), Gap (0.3 mm), Current (90 A), Pon (130 ms), and Poff (100 ms), an optimal range of TWR obtain.

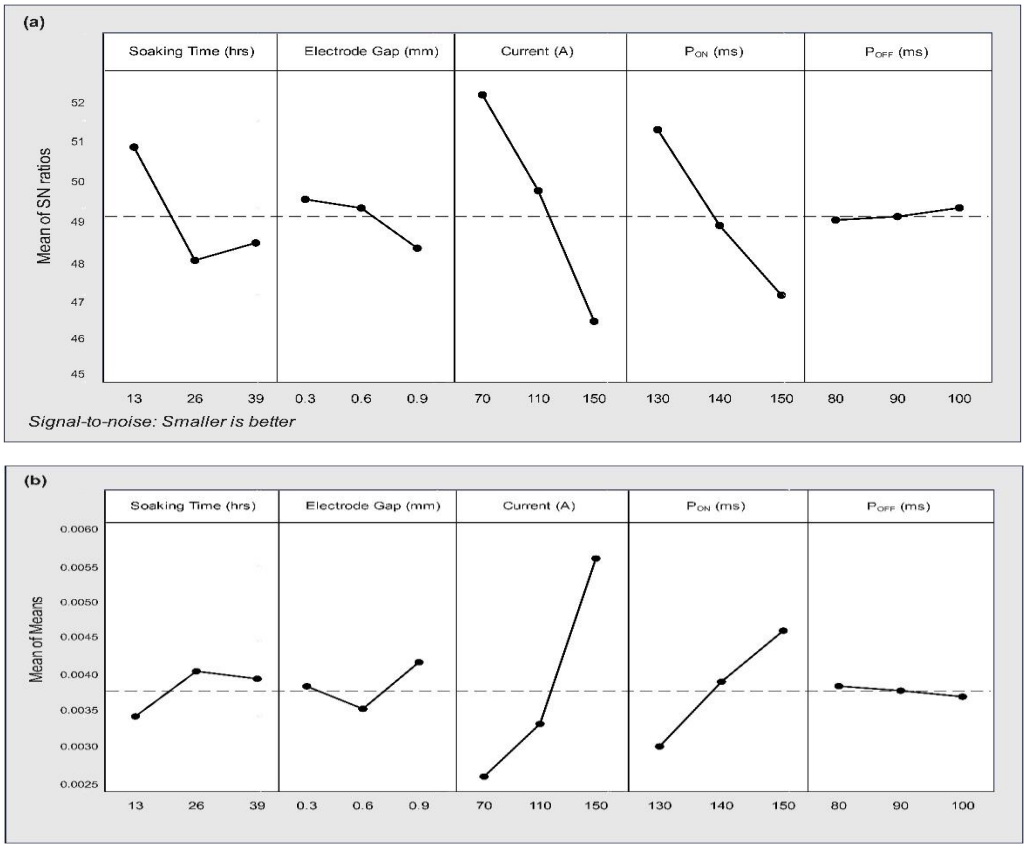

Figure 6. (a)TW rate main effect plot – SN ratio,(b)TW rate main effect plot - means.

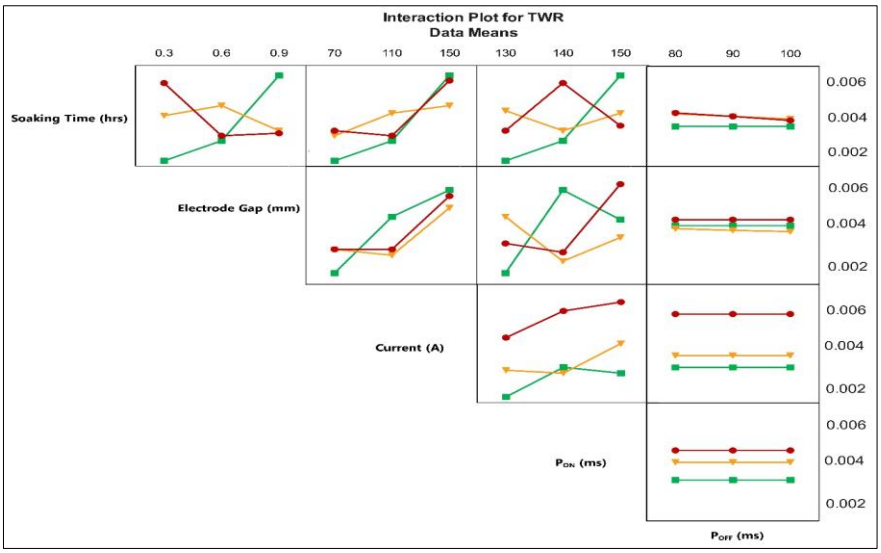

Figure 7. TWR's interaction plot.

5.4 Surface Roughness (Ra)

Ra is the measurement used to surface size the fineness of the imperfections on a machined surface. If the Ra value is high, the surface is rough, whereas a low number implies a smooth one. Three aspects make up the overall roughness of a surface: (i) the roughness itself, ii) the waviness of the surface, and iii) the shape of the ridges and valleys—microscopic craters connected to random spark discharge between tool and W/P, the character created by electrical discharge machining. Crater formation over the machined surface is proportional to the discharge energy's most incredible intensity. A more profound crater formation from higher discharge energy leads to a higher Ra value but also causes a higher MR rate. Table 15 displays an ANOVA for the SN ratio of Ra. According to this data, the current input parameter has the highest F value, followed by the transistor's gap and state.

Table 16 displays the SN response, which ranks the elements impacting the Ra of the machined surface by delta value and indicates how those parameters have an effect. In that order, Gap, Current, and SoT are the three most critical influencing parameters. Means-based analysis of variance (ANOVA) results indicates in Table 17; that a high F value implies that a given component has the most significant impact on Ra. The more considerable F value of gaps significantly impacts the Ra quality. Table 18 lists the delta value to rank the influencing factors: (i) Gap, (ii) Current, and (iii) SoT. There are various bumps and ridges on the machined surface because of the influence of the input parameters. Numerous inputs interact to produce the final roughness of a character. Values of surface roughness on the lower end of the spectrum suggest a smooth surface, while higher values imply more significant surface irregularities. The affecting SR factor for the machined surface predictsusing analysis. Figures 8 (a & b) illustrate the correlation between Ra and the input parameters, the SN ratio, and mean of means. The surface roughness interaction plot indicates in Figure 9. Ra attains to be best at anSoT(13 Hrs), Gap(0.3 mm), Current(90 A), Pon(130 ms), and Poff(100 ms).

Table 15. ANOVA for S/N ratios ofSurface Roughness.

Source	DF	Seq SS	Adj SS	Adj MS	F	P
A	2	1.1961	1.1961	0.59791	1782.22	0
B	2	18.6249	18.6249	8.80789	26242.3	0
C	2	3.3181	3.3181	1.65872	4942.61	0
D	2	0.4162	0.4162	0.20773	619.62	0
E	2	0.0079	0.0079	0.00392	12.67	0.001
Residual Error	16	0.0055	0.0055	0.00036		
Total	26	23.5687				

Table 16. S/N ratio's response table for Surface Roughness.

Level	A	B	C	D	E
1	−13.31	−12.39	−13.18	−13.38	−13.48

2	−13.79	−13.68	−13.22	−13.7	−13.43
3	−13.31	−14.29	−13.94	−13.32	−13.42
Delta	0.46	1.95	0.78	0.29	0.05
Rank	3	1	2	4	5
Smaller is better					

Table 17. ANOVA for means ofSurface Roughness.

Source	DF	Seq SS	Adj SS	Adj MS	F	P
A	2	0.39263	0.39263	0.19628	1615.21	0
B	2	4.97233	4.97233	2.48612	20460.27	0
C	2	0.96815	0.96815	0.48361	3979.71	0
D	2	0.09898	0.09898	0.04951	407.28	0
E	2	0.00235	0.00235	0.00118	9.63	0.002
Residual Error	16	0.00196	0.00196	0.00013		
Total	26	6.4364				

Table 18. Mean's response table for surface roughness.

Level	A	B	C	D	E
1	4.658	4.148	4.581	4.698	4.732
2	4.889	4.828	4.59	4.802	4.717
3	4.617	5.19	4.987	4.658	4.709
Delta	0.273	1.035	0.407	0.145	0.023
Rank	3	1	2	4	5

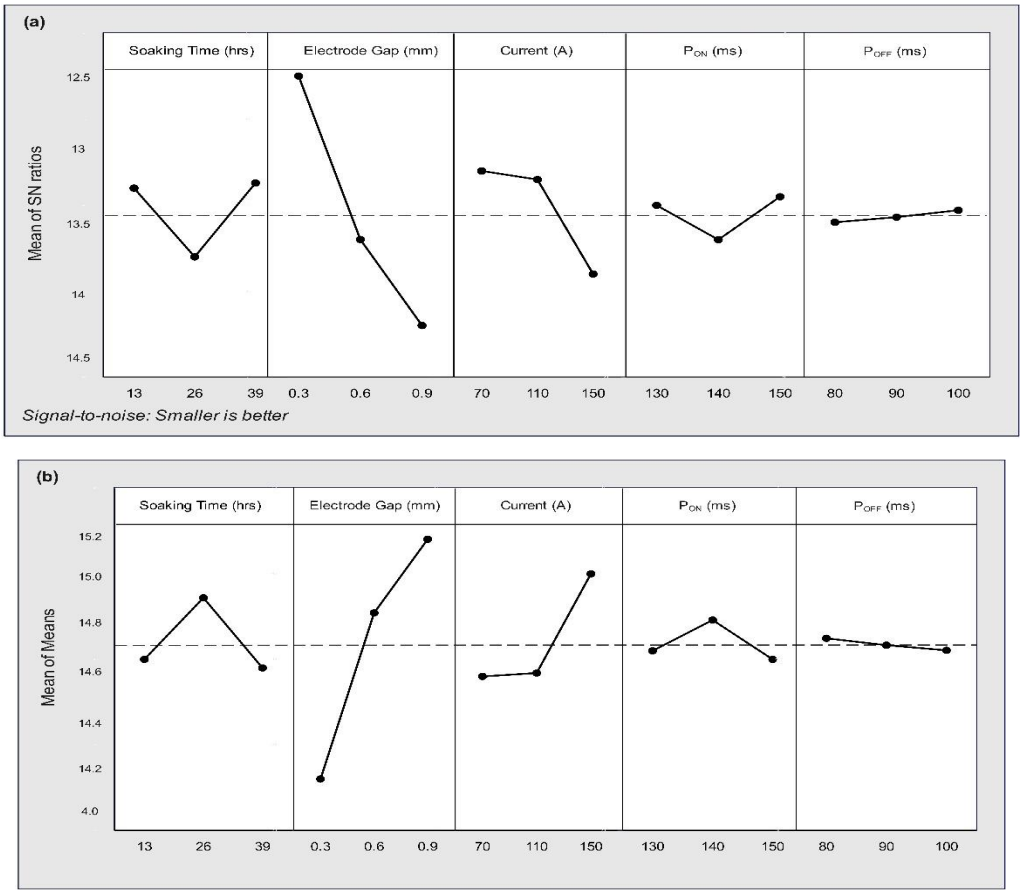

Figure 8. The main effect plot is(a)SN ratioand (b)means.

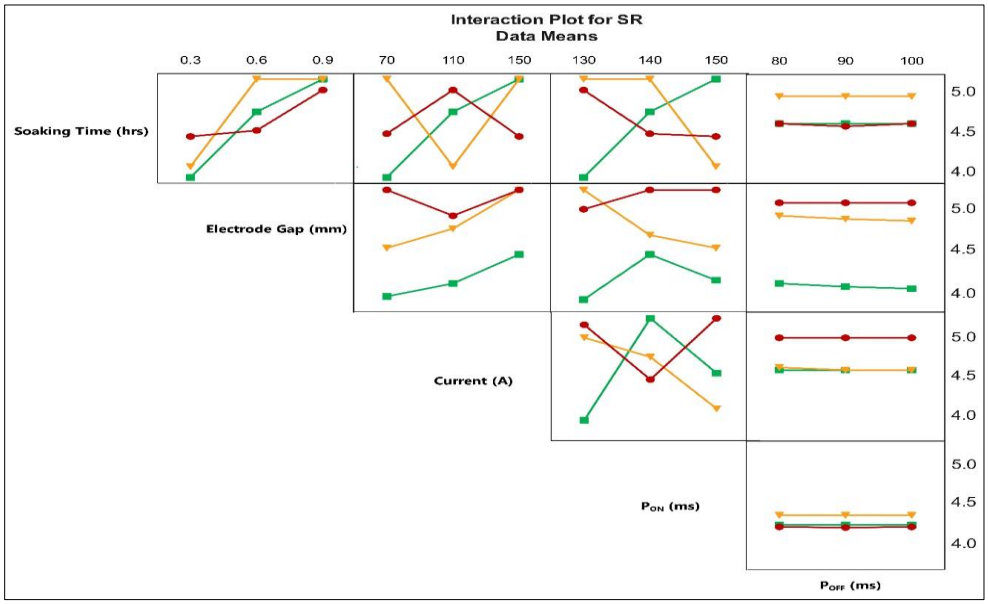

Figure 9. Surface Roughness's interaction plot

6. CONCLUSIONS

This research studied the effects of various processing parameters on ED machining of composite material manufactured from AA6063. The SN ratio, ANOVA, and F-test result all point to an increase in MR rate due to the higher Current and Pon. The low MR rate directly resulted from the standard pulse current created by the discharge. However, the increased peak current discharge energy results in a deeper cavity forming. The time required for Poff in the machining zone increases with the cavity's depth because more debris eradicates. Process factorsoptimize to achieve maximum MR throughout. While the current and Pon both increased, the TW rate decreased. When the W/P ratio changes, the tool electrode wears down because of the dynamic process between the two. The settings (pulse on duration, low Current, and Poff) prevent further erosion of the tool's surface by depositing broken carbon particles from the dielectric fluid. Ra instructed to improve in Gap and Current, which resulted in a high-energy pulse that cratered the machined surface, resulting in a subpar finish. Using the Taguchi approach, researchers could independently optimize the MR rate, the TW rate, and the value of Ra; the resulting optimal values are 0.6221, 0.0015, and 3.918.

REFERENCES

[1] R. Anil Kumar and N. Radhika, “Enhancement of mechanical and wear properties of tungsten carbide coated AA 6063 alloy using detonation gun technique,” *Transactions of the Institute of Metal Finishing*, vol. 96, no. 4. pp. 212–219, 2018. doi: 10.1080/00202967.2018.1477265.

[2] R. P. Kumar and S. Arul, “Improving the wear and corrosion resistance of nickel aluminium bronze by deep cryogenic treatment,” *Mater. Today Proc.*, vol. 46, pp. 4915–4918, 2019, doi: 10.1016/j.matpr.2020.10.334.

[3] P. Sonia, V. Verma, K. K. Saxena, N. Kishore, and R. S. Rana, “Effect of cryogenic treatment on mechanical properties and microstructure of aluminium 6082 alloy,” *Mater. Today Proc.*, vol. 26, pp. 2248–2253, 2019, doi: 10.1016/j.matpr.2020.02.488.

[4] N. Vasudevan, G. B. Bhaskar, T. S. Rao, and M. Mohandass, “Mechanical properties of cryogenically treated AA5083 friction stir welds,” *Mater. Test.*, vol. 6, no. 12, pp. 1129–1134, 2019, doi: 10.3139/120.111430.

[5] B. V Sunil Kumar, N. V Londe, A. O. Surendranathan, and K. Anilas, “Study on Mechanical & Cryogenic Properties of Carbon Epoxy Composites,” in *IOP Conference Series: Materials Science and Engineering*, 2018, vol. 376, no. 1. doi: 10.1088/1757-899X/376/1/012047.

[6] A. Viceré, M. Cabibbo, C. Paoletti, G. Roventi, and T. Bellezze, “Analysis of corrosion behaviour of aluminium alloy AA6012 samples processed by ECAP and cryogenic treatment ,” *Metall. Ital.*, vol. 110, no. 2, pp. 25–33, 2018, [Online]. Available: https://www.scopus.com/inward/record.uri?eid=2-s2.0-85044827557&partnerID=40&md5=e193e1cd8254080074198964c24bb771

[7] H. Nazarian, M. Krol, M. Pawlyta, and S. E. Vahdat, “Effect of sub-zero treatment on fatigue strength of aluminum 2024,” *Mater. Sci. Eng. A*, vol. 710, pp. 38–46, 2018, doi: 10.1016/j.msea.2017.10.072.

[8] M. Araghchi, H. Mansouri, R. Vafaei, and Y. Guo, “A novel cryogenic treatment for reduction of residual stresses in 2024 aluminum alloy,” *Mater. Sci. Eng. A*, vol. 689, pp. 48–52, 2017, doi: 10.1016/j.msea.2017.01.095.

[9] N. Kaushik and S. Singhal, “Examination of wear properties in dry-sliding states of SIC strengthened al-alloy metal matrix composites by using taguchi optimization approach,” *Int. J. Appl. Eng. Res.*, vol. 12, no. 20, pp. 9708–9716, 2017, [Online]. Available: https://www.scopus.com/inward/record.

uri?eid=2-s2.0-85040678374&partnerID=40&md5=52aa69bf84c7ebd75c6a7af991b073ad

[10] D. Yanagida *et al.*, "Electrical discharge machining using copper electrode made by additive manufacturing," in *Procedia CIRP*, 2020, vol. 95, pp. 449–453. doi: 10.1016/j.procir.2020.02.293.

[11] J. Kumar, S. Majumder, A. K. Mondal, and R. K. Verma, "Influence of rotation speed, transverse speed, and pin length during underwater friction stir welding (UW-FSW) on aluminum AA6063: A novel criterion for parametric control," *Int. J. Light. Mater. Manuf.*, vol. 5, no. 3, pp. 295–305, 2022, doi: 10.1016/j.ijlmm.2022.03.001.

[12] M. Meignanamoorthy *et al.*, "Effect of Nanoaluminium Nitride Ceramic Particles on Microstructure, Mechanical Wear, and Machining Behavior of Al-Si-Mg Alloy Matrix Composites Produced by Bottom Pouring Type Stir Casting Route," *J. Nanomater.*, vol. 2022, 2022, doi: 10.1155/2022/5013914.

[13] K. Ravi Kumar, N. Soms, S. Selvakumar, and V. S. Sreebalaji, "Investigation and optimization of machining through hole by abrasive water jet machining in AA6063/Bagasseash/TiN hybrid composites," *Mater. Manuf. Process.*, vol. 36, no. 15, pp. 1813–1827, 2021, doi: 10.1080/10426914.2021.1954194.

[14] M. Iwai, W. Chen, P. Chen, B. Lin, and K. Suzuki, "Proposal of coarse grain PCD with fine particles of boron-doped diamond mixed in," 2016. [Online]. Available: https://www.scopus.com/inward/record.uri?eid=2-s2.0-84984633641&partnerID=40&md5=143a6690323ba21fb521d1fae3a1e67e

[15] I. Dokmanic, R. Parhizkar, J. Ranieri, and M. Vetterli, "Euclidean Distance Matrices: Essential theory, algorithms, and applications," *IEEE Signal Process. Mag.*, vol. 32, no. 6, pp. 12–30, 2015, doi: 10.1109/MSP.2015.2398954.

[16] A. Abdullah, A. Azman, and B. M. Khirulrizwan, "Optimization of surface roughness by using different cutting tools for aluminum Alloy 6063," *J. Comput. Theor. Nanosci.*, vol. 17, no. 2–3, pp. 961–966, 2020, doi: 10.1166/jctn.2020.8750.

[17] A. Daniel Das, S. N. Vijayan, and N. Subramani, "Investigation on welding strength of fsw samples using taguchi optimization technique," *J. Crit. Rev.*, vol. 7, no. 9, pp. 179–182, 2020, doi: 10.31838/jcr.07.09.36.

[18] S. M. Senthil, R. Parameshwaran, S. Ragu Nathan, M. Bhuvanesh Kumar, and K. Deepandurai, "A multi-objective optimization of the friction stir welding process using RSM-based-desirability function approach for joining aluminum alloy 6063-T6 pipes," *Struct. Multidiscip. Optim.*, 2020, doi: 10.1007/s00158-020-02542-2.

[19] R. K. Tayal, S. Kumar, A. Mondal, and S. Jambhale, "Experimental Investigation and Parametric Optimization of AA6063/AA6351 Alloys Bimetallic Prepared by Vacuum-Assisted Lost Foam Compound Casting Process," *Int. J. Met.*, vol. 14, no. 1, pp. 243–256, 2020, doi: 10.1007/s40962-019-00349-6.

[20] S. Saravanan, V. Vijayan, A. V Balan, T. Sathish, and A. Parthiban, "Exploration on surface roughness in abrasive water jet cutting of AA6063-TiC composites for vehicle structural applications," *Int. J. Veh. Struct. Syst.*, vol. 11, no. 4, pp. 417–421, 2020, doi: 10.4273/ijvss.11.4.15.

[21] M. Y. Reddy and K. Rajanikanth, "An experimental investigation and process parameters optimization of friction stir welded dissimilar alloys," *Int. J. Mech. Prod. Eng. Res. Dev.*, vol. 9, no. 4, pp. 919–926, 2019, doi: 10.24247/ijmperdaug201993.

[22] O. P. Singh, G. Kumar, and M. Kumar, "Multi performance optimizationof shoulder

milling process parameters of AA6063 T6 aluminium alloy by taguchi based GRA," *Int. J. Innov. Technol. Explor. Eng.*, vol. 8, no. 10 Special Issue, pp. 420–425, 2019, doi: 10.35940/ijitee.J1078.08810S19.

[23] P. Sahoo, M. P. Satpathy, V. K. Singh, and A. Bandyopadhyay, "Performance evaluation in CNC turning of AA6063-T6 alloy using WASPAS approach," *World J. Eng.*, vol. 15, no. 6, pp. 700–709, 2018, doi: 10.1108/WJE-06-2017-0127.

[24] B. Stalin, P. R. Kumar, M. Ravichandran, and S. Saravanan, "Optimization of wear parameters and their relative effects on stir cast AA6063-Si3N4 Composite," *Materials Research Express*, vol. 5, no. 10. 2018. doi: 10.1088/2053-1591/aad99c.

[25] P. A. Sylajakumari, R. Ramakrishnasamy, and G. Palaniappan, "Taguchi grey relational analysis for multi-response optimization of wear in co-continuous composite," *Materials (Basel).*, vol. 11, no. 9, 2018, doi: 10.3390/ma11091743.

[26] P. Sureshkumar and V. C. Uvaraja, "Effect of ceramic and metallic reinforcement on mechanical, corrosion, and tribological behavior of aluminum composite by adopting design of experiment through Taguchi technique," *J. Tribol.*, vol. 140, no. 5, 2018, doi: 10.1115/1.4039527.

[27] W. Chen, M. Iwai, and K. Suzuki, "EDM machinabilities of EC-PCD using ultrasonic assisted EDM and bipolar pulse current EDM," *Advanced Materials Research*, vol. 1017. pp. 782–787, 2014. doi: 10.4028/www.scientific.net/AMR.1017.782.

[28] W. Chen, M. Iwai, S. Ninomiya, and K. Suzuki, "Material properties of a new PCD made of boron doped diamond particles," *Advanced Materials Research*, vol. 1017. pp. 154–159, 2014. doi: 10.4028/www.scientific.net/AMR.1017.154.

[29] W. Chen, S. Ninomiya, S. Nochi, M. Iwai, and K. Suzuki, "Wire-EDM properties of EC-PCD made up of boron doped diamond particles," *Advanced Materials Research*, vol. 1017. pp. 770–775, 2014. doi: 10.4028/www.scientific.net/AMR.1017.770.

[30] M. A. Madhloom, A. H. Ataiwi, and J. J. Dawood, "Influence of cryogenic treatment on hardness, tensile properties, and microstructure of aluminum alloy AA6061," *Mater. Today Proc.*, vol. 60, pp. 2157–2161, 2022, doi: 10.1016/j.matpr.2022.02.131.

[31] S. Ma, R. Su, K. Wang, Y. Yang, Y. Qu, and R. Li, "Effect of Deep Cryogenic Treatment on Wear and Corrosion Resistance of an Al–Zn–Mg–Cu Alloy," *Russ. J. Non-Ferrous Met.*, vol. 62, no. 1, pp. 89–96, 2021, doi: 10.3103/S1067821221010144.

[32] N. Kaushik and S. Singhal, "Optimization of wear properties in aluminum metal matrix composites using hybrid taguchi-GRA-PCA," *Int. J. Performability Eng.*, vol. 14, no. 5, pp. 857–870, 2018, doi: 10.23940/ijpe.18.05.p4.857870.

[33] N. Kaushik and S. Singhal, "Hybrid combination of Taguchi-GRA-PCA for optimization of wear behavior in AA6063/SiCp matrix composite," *Prod. Manuf. Res.*, vol. 6, no. 1, pp. 171–189, 2018, doi: 10.1080/21693277.2018.1479666.

[34] G. E. Abrosimova, N. A. Volkov, and A. S. Aronin, "Restoration of the Structure of Amorphous Alloys and Partially Crystalline Alloys Using Cryogenic Thermocycling," *Inorg. Mater.*, vol. 56, no. 15, pp. 1467–1470, 2020, doi: 10.1134/S0020168520150029.

[35] W. Zhang, K. Li, Q. Xiang, Y. Ren, Q. Li, and K. Qiu, "The rejuvenation and relaxation around the glass transition of a Ce-based metallic glass controlled by annealing, quenching and cryogenic treatments," *J. Non. Cryst. Solids*, vol. 548, 2020, doi: 10.1016/j.jnoncrysol.2020.120334.

[36] W. Zhang, Q. C. Xiang, C. Y. Ma, Y. L. Ren, and K. Q. Qiu, "Relaxation-to-rejuvenation transition of a Ce-based metallic glass by quenching/cryogenic treatment performed at sub-Tg," *J. Alloys Compd.*, vol. 825, 2020, doi: 10.1016/j.jallcom.2020.153997.

[37] S. K. Gupta, K. N. Pandey, and R. Kumar, "Experimental modelling and genetic algorithm-based optimisation of friction stir welding process parameters for joining of dissimilar AA5083-O and AA6063-T6 aluminium alloys," *Int. J. Mater. Prod. Technol.*, vol. 56, no. 3, pp. 253–270, 2018, doi: 10.1504/IJMPT.2018.090818.

[38] U. Koklu, "The drilling machinability of 5083 aluminum under shallow and deep cryogenic treatment," *Emerg. Mater. Res.*, vol. 9, no. 2, pp. 323–330, 2020, doi: 10.1680/jemmr.19.00127.

[39] S. Satpathy and A. Ghosh, "On material removal mechanism in high speed single grit scratchgrinding of cryo-treated Al2024-T351 aluminium alloy," *Materials Science Forum*, vol. 1009 MSF. pp. 123–128, 2020. doi: 10.4028/www.scientific.net/MSF.1009.123.

[40] K. Arunkarthikeyan, K. Balamurugan, M. Nithya, and A. Jayanthiladevi, "Study on Deep Cryogenic Treated-Tempered WC-CO insert in turning of AISI 1040 steel," in *Proceedings of 2019 International Conference on Computational Intelligence and Knowledge Economy, ICCIKE 2019*, 2019, pp. 660–663. doi: 10.1109/ICCIKE47802.2019.9004422.

[41] Chetan, S. Ghosh, and P. V Rao, "Comparison between sustainable cryogenic techniques and nano-MQL cooling mode in turning of nickel-based alloy," *J. Clean. Prod.*, vol. 231, pp. 1036–1049, 2019, doi: 10.1016/j.jclepro.2019.05.196.

[42] X. Ma, Y. Zhao, X. Zhao, J. Nie, H. Chen, and X. Liu, "Mechanisms on the outstanding high temperature plasticity of AlNp/Al–0.4Cu composites induced by cryogenic treatment," *J. Alloys Compd.*, vol. 770, pp. 755–764, 2019, doi: 10.1016/j.jallcom.2018.08.051.